The Detection of Blotches in Old Movies

Xu Li[*], Ranran Zhang[†], Yi Zhang[‡]
[*] School of Mathematical Sciences, Nankai University, Tianjin, China
E-mail: lixu@nankai.edu.cn
[†]Shanghai Fudan-holding Hualong Microsystem Techology Co. Ltd, Shanghai, China
E-mail: automaticzrr@163.com
[‡] School of Computer Software, Tianjin University, Tianjin, China
E-mail: yizhang@tju.edu.cn

***Abstract*—Blotch detection is one of the most important steps in the old movies restoration. The existing blotch detection algorithms get higher correct detection rates by reducing the threshold value. However, the corresponding higher false alarms affect the following correction results directly. To maximize the ratio between correct detections and false alarms, an improved blotch detection algorithm based on simplified rank-ordered difference is proposed in this paper. The improved algorithm can achieve the most appropriate threshold for the different blotches in one frame by introducing dual-step adaptive multi-threshold; meanwhile the employment of texture matching avoids the possible deviation caused by motion vector estimation in the regions with blotches. Performance evaluation is taken to the image sequences with both real blotches and artificially corrupted ones separately. The experimental results indicate that our algorithm can achieve higher correct detection rates and lower false alarms.**

I. INTRODUCTION

There are numerous kinds of artifacts in old movies especially in films, blotches are common ones. Blotch is known as dark or bright spot in the film frame which make the movie less valuable in both researching and watching. To restore the blotches without distorting the unaffected regions in the old movies, the locations of the blotches must be identified correctly, and this process is called blotch detection.

Blotches have three characteristic properties that can be exploited by blotch detection algorithms. Firstly, blotches are temporally independent; therefore hardly ever occur at the same spatial locations in the successive frames. Secondly, the intensity of a blotch is significantly different from its neighboring uncorrupted intensities. Finally, blotches form coherent regions in a frame as opposed to spatiotemporal shot noise [1]. Above three characteristics are exploited in various detectors. The evaluation of these detectors is the ratio between the correct detections and the false alarms.

II. BACKGROUNDS

Blotch detection algorithms are generally classified into two categories: object based method and pixel based method. The former one exploits the spatial coherence within blotches. The latter one assesses each pixel whether it is the part of a blotch independently using information [2]. Earliest detector was proposed by Storey in 1985 [3, 4]. This algorithm compares the differences between frames to a predefined threshold to locate the blotches directly. In 1992, A. C. Kokaram and P.J.W. Rayner employed motion vector compensation to the visualized method which is known as SDI (Spike Detection Index) detector[5]. After that, SDIa (Spike detection Index-a) detector and SDIp (Spike Detection Index-p) detector are proposed [2]. These three detectors built on similar basis and their detection results are approachable [2]. The core idea of MRF detector [6-8] is maximizing the probability between the pre-post-frame and current frame. Usually, MRF detector can achieve better detection accuracy at the cost of high computation. More recently, M. J. Nadenau and S. K. Mitra proposed ROD (Rank-Ordered Difference) detector [9] based on SDI detector. The ratio between the correct detections and the false alarms outperforms above mentioned detectors based on threshold because it is less easily affected by predefined threshold. In 1999, P. M. B. van Roosmalen simplified ROD detector which is known as S-ROD (Simplified Rank-Ordered Difference) detector [10] and employed a series of post-processing to improve the detection performance. It is proved that S-ROD detector is the best one in the existing detectors in Ref. [10]. In addition, S. Tilie, L. Laborelli and I. Bloch proposed a novel method based on a contrario decision theory to improve the blotch detection [2]. This method adopts the concept of probability of accidental occurrence which has been extended to image analysis by Desolneux [11], and successfully applies to the detection of alignments [12] and moving objects [13]. However, this method can only improve the ratio between the correct detection and the false alarms by reducing the false alarms.

III. THE PROPOSED BLOTCH DETECTOR

As mentioned above, S-ROD detector is superior in both detection accuracy and computational cost. However, the drawbacks of S-ROD detector are also obvious. One of them is that inaccurate results may be caused by motion estimation in the regions with blotches. And another one is that different objects of blotches may be incompletely detected using uniform threshold in one frame. To overcome the drawbacks,

an improved blotch detector based on texture matching and dual-step adaptive multi-threshold is proposed in this paper. Firstly, the initial blotches are detected in the frame by S-ROD detector. According to the position information of each initial blotch, the most matching blotches in pre-frame and post-frame are found by texture matching. Secondly, the S-ROD detection is performed iteratively with decreasing threshold. In each iteration, two different decreasing threshold offsets are used, and two detection results are compared with each other. The better result is used as the input for the next iteration. The most appropriate result is obtained when meeting the predefined condition of convergence.

A. Initial detection

To avoid the possible false alarms caused by S-ROD detector in the condition of extreme value, the discriminant is defined as:

$$S(i)=\begin{cases}1 & if\ \left|Z(i)-\min(p_k)\right|>T_1\ \ and\ \ \left|\max(p_k)-Z(i)\right|>T_1\\ 0 & otherwise\end{cases} \tag{1}$$

Where Z(i) denotes the intensity of a pixel at a spatial location z^T = (x, y) in frame n. T_1 is the predefined threshold. And p_k forms a set of six reference pixels, obtained from spatially co-sited pixels and their vertical neighbors in motion compensated previous and next frames. Fig. 1 shows the selection of reference pixels set p_k. While *S(i) = 1, x(k)* is detected as blotch.

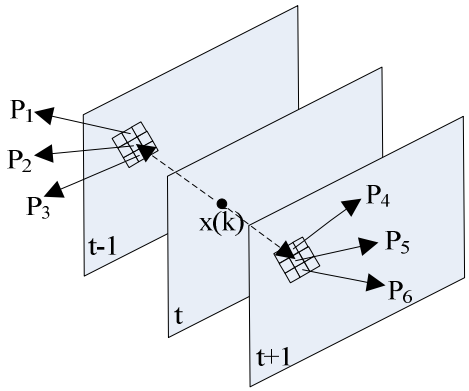

Fig. 1 The selection of reference pixels p_k

B. Texture matching

To avoid the possible inaccurate results brought by motion estimation in the region with blotches, texture matching is introduced to search the most matching blocks in pre-frame and post-frame. To insure the result of texture matching, the blocks have to be resized (see Fig.2 (b)) to contain more valid texture information, which insures better matching results. There will be intersections between the resized blocks. All the superposed blocks are merged into one block(see Fig.2 (c)). To void the unlimited combination, the superposed blocks are merged only once.

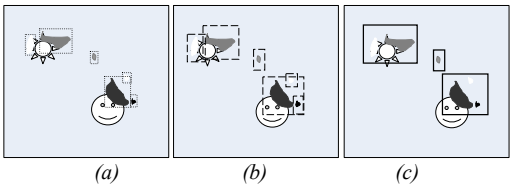

Fig. 2 The definition of blocks (a)the original definition of blocks (b)the resized blocks (c)the merged blocks

To improve the efficiency of the detector, SAD (Sum of Absolute Differences) is used to measure the similarity between the blocks. The definition of SAD is as below:

$$SAD(\psi_p,\psi_q)=\sum_{i=0}^{N-1}\sum_{j=0}^{N-1}\left|I_t(x+i,y+j)-I_{t-1}(m+i,n+j)\right| \tag{2}$$

$$\psi_q=\arg\min_{\psi_q\in\phi} SAD(\psi_p,\psi_q) \tag{3}$$

Where *x*, *y* and *m*, *n* are discrete spatial coordinates of the top left point of the block ψ_p and the block ψ_q, N is the size of the block, ϕ is the searching region. Eq. (3) indicates that we will take the best approximate match of the block with smallest SAD value.

To verify that texture matching can improve detection rate, the local detection results are compared in Fig. 3. Fig. 3(a) is the 4th block of blotches in the 2nd frame of Mobile and Calendar sequence with 6 artificial blotches (taking the boxes in Fig. 4 for reference). The S-ROD detector shows higher false alarms caused by inaccurate motion estimation (see the red circles in Fig. 3(d)). In addition, the blotch cannot be detected completely in the region where the pixel color is similar to the color of the blotch (see the blue box in Fig. 3(d)). Using our method, the probability of wrongly detection as blotches is reduced (see Fig. 3(e)).

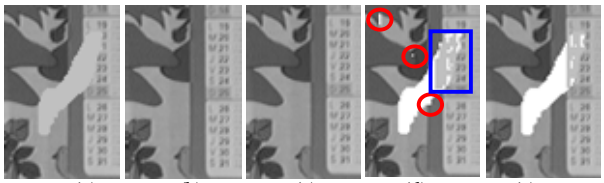

Fig. 3 The local detection results based on texture matching (a) the block of artificial blotch (b) the matching block in previous frame (c) the matching block in next frame (d) the detection result of the S-ROD detector based on motion vector estimation (e) the detection result based on texture matching

C. Dual-step adaptive multi-threshold

To further improve the correct detection rate, each blotch is detected independently by dual-step adaptive multi-threshold. The iteration steps are:

a) Define the initial detection result as *W* which is obtained when threshold T_1 = 15.

b) Define $T_2 = T_1 - \Delta_1$, $T_3 = T_1 - \Delta_2$ (Δ_1=2, Δ_2=5 in our experiment).

c) Detect the blotch blocks using threshold T_2 and T_3 and record the detection results as W_1 and W_2 respectively.
d) Compare W_1 and W_2 and take the better one as W. T_1 is substitute for with corresponding threshold.
e) Iterate step *b)- d)* until the condition of convergence is satisfied. W is the final detection result.

Fig. 5 is a pixel-based sketch map of the detection step. □,□,■ are respectively the pixels which are the real image, the pixels which are marked as blotches and pixels which are the real blotches.

Fig. 4 The 2nd frame of Mobile and Calendar sequence with artificial blotches

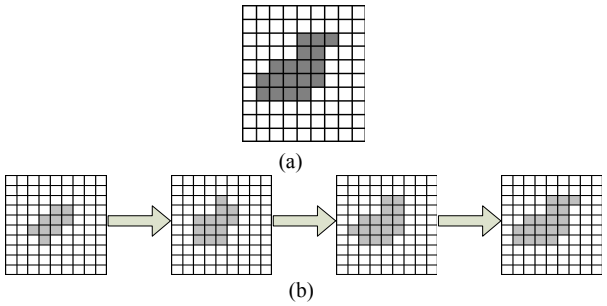

Fig. 5 The pixel based iterative detection results (a) the image with blotches (b) the procedure of iterative detection

D. The condition of convergence

In the iteration, the condition of convergence of step *e)* influences the efficiency and accuracy of the blotch detection. To define the condition of convergence more accurately, we compare the results of each iteration step. Table 1 shows the results of detection results of 6 blotches in Fig. 4 while T_1 is 15, 13, 10, 8, and 5 respectively.

From the table 1 we can see that the correct detection rate of the 3rd block of blotch is almost 100%. And the false alarms increase rapidly once the threshold reduces. In this experiment, the most accurate detection result of 3rd block of blotch is obtained when $T_1=15$. Similarly, the detection result of 2nd block of blotch is the best when $T_1=10$. However, for the other four blocks of blotches, the ratios between correct detection results and false alarms are acceptable at most threshold levels. It is necessary to define different threshold for each block of blotch in one frame.

Fig. 6 shows the pixel-based iterative detection results, where □ and ▒ are respectively the real pixel of image and the pixel marked to be part of blotch, ▒ are the pixels next to ▒ in previous iterative step, and ■ are the pixels which are not next to ▒ in previous iterative step.

We define λ as:

$$\lambda = \frac{N_\alpha \cdot \sum_{i=1}^{N_\alpha} \sqrt{(x_i^\alpha - x_0)^2 + (y_i^\alpha - y_0)^2}}{N_\beta \cdot \sum_{i=1}^{N_\beta} \sqrt{(x_i^\beta - x_0)^2 + (y_i^\beta - y_0)^2}} \quad (4)$$

In Eq. (4), N_α and N_β are the numbers of new ■ and ▒ respectively. (x_0, y_0) denotes the coordinate of the center pixel in the region ▒. (x_i^α, y_i^α) and (x_i^β, y_i^β) are respectively the coordinates of i^{th} pixel in the region ■ and ▒. Additionally, we define $\lambda = N_\alpha \cdot \sum_{i=1}^{N_\alpha} \sqrt{(x_i^\alpha - x_0)^2 + (y_i^\alpha - y_0)^2}$ while N_β=0.

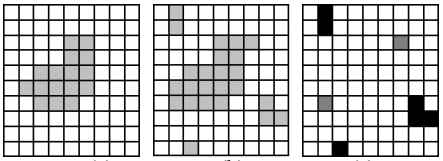

Fig. 6 The pixel-based iterative detection results and the differential result (a) the detection result in *n* step (b) the detection result in *n+1* step (c) the difference between (a) and (b).

For deciding the convergence of iteration, we compute the values of λ when $T_2 = T_1 - \Delta_1$ and $T_3 = T_1 - \Delta_2$ respectively. The results are denoted with λ_1 and λ_2. If $\lambda_2 \geq \lambda_1$, the iteration is resumed, otherwise the step size is Δ_1 in the next iteration. We compare the values of λ when the iteration time is *n* and *n-1*. If $\lambda_n \geq \lambda_{n-1}$, the iteration is continued with updated threshold, otherwise the detection result in iteration *n-1* is the final one.

IV. EXPERIMENTAL RESULTS

We use three different image sequences with blotches in our experiments. The first one is an image sequence in a real degraded film. The image resolution is 512*512(see Fig. 7(a)). The second one is an image sequence which is corrupted with random blotches. The image resolution is 256*256 (see Fig. 8(a)). The last one is a set of artificial frames with resolution 512*400(Fig. 9(a)). The input sequences above are all taken from CD-ROM in [2]. Besides, the detection results in Fig. 7(b)-(c) are also taken from CD-ROM in [2]. All the other experiment results are performed using MATLAB 7.0 running on a core 1.6GHz and 2.0G memory PC.

From the detection results of real degraded image sequence Bay (Fig. 7), we can see that the detection results obtained by our detector are visually superior to the other detectors in both detection accuracy and false alarms.

To the 2nd type of image sequence Western, the corrupted blotches are random in pixel value, location and size. We

label the blotches which are obviously different in detection results (see the red rectangle in Fig. 8). We can see that the correct detection results obtained by our detector are outstanding when $T_1 = 30$.

In Fig. 9, the blotches are labeled in blue rectangle in Fig. 9(b) and (c). These six corrupted blotches are located in or through certain regions where the pixel values are similar to the blotch values. So they are more difficult to be detected.

Receiver Operating Characteristic (ROC) curve is used to compare the detection results obtained by our detector and S-ROD post detector (see Fig. 10). The curves of two detectors are generated by measuring detection accuracy for threshold varying from 6 to 36. For the random corrupted image sequence Mobile and Calendar (Fig. 10(a)), our detector has about 3 times less false detections than S-ROD post detector for a correct rate of 80%. For the artificial frames, it can be seen from Fig. 10 (b) that our detector performs outstanding, retaining more than 60% correct detection rate with less than 1% false alarm rate.

V. CONCLUSION

In this paper, an improved blotch detector based on texture matching and dual-step adaptive multi-threshold is proposed. To maximize the ratio between correct detection and false alarms, texture matching is used to find out the most matching blocks in the pre-frame and post-frame. It can overcome the drawback of possible inaccurate matching results causing by motion vector estimation in these blocks. Based on the optimal results of texture matching, dual-step adaptive multi-threshold is employed. The threshold of each blotch block is independent. It can avoid over-detection and under-detection with single threshold. The experimental results prove that our detector can improve the detection accuracy.

ACKNOWLEDGMENT

This work was financially supported by the Key Projects in the Science and Technology Pillar Program of Tianjin, under Grant No. 11ZCKFGX01200.

REFERENCES

[1] Alan Bovik, "Handbook of Image and Video Processing (second edition)," *Publishing House of Electronics Industry*, 2006.

[2] A. C. Kokaram, "Motion Picture Restoration: Digital Algorithms for Artifact Suppression in Degraded Motion Picture Film and Video," *Springer-Verlag*, 1998.

[3] R. Storey, "Electronic Detection and Concealment of Film Dirt," UK patent 2139039, 1984.

[4] R. Storey, "Electronic detection and Concealment of Film Dirt," *SMPTE Journal,* 1985, vol. 5, pp. 642-653

[5] A. C. Kokaram, P. J. W. Rayner, "A System for the Removal of Impulsive Noise in Image Sequences," *International Conference on SPIE Visual Communications in Image Processing*. Boston, 1992.

[6] A. C. Kokaram, Robin D. Morris, W. J. Fitzgerald et al., "Detection of Missing Data in Image Sequences," l*EEE Trans. Image Processing,* 1995, vol. 11, pp.1496-1501.

[7] R. Bornard, "Probabilistic Approaches for the Digital Restoration of Television Archives," *Paris: Ecole Centrale Paris,* 2002.

[8] M. N. Chong, P. Liu, W. Goh, et al., "A New Spatio-Temporal MRF Model for the Detection of Missing Data in Image Sequences," *IEEE International Conference on Acoustics, Speech, and Signal Processing,* Munich: 1997.

[9] M. J. Nadenau, S. K. Mitra, "Blotch and Scratch Detection in Image Sequences Based on Rank Ordered Differences," *5th International Workshop on Time-Varying Image Processing and Moving Object Recognition*, Florence: 1996.

[10] P. M. B. van Roosmalen, "Restoration of Archived Film and Video," *Delft: Delft University of Technology*, 1999.

[11] J. Biemond, P. M. B. van Roosmalen and R. L. Lagendijk, "Improved Blotch Detection by Post-processing," *IEEE International Conference on Acoustics,* Speech, and Signal Processing, 1999, vol.6, pp. 3101-3109.

[12] P. M. B. van Roosmalen, "Technical report for ina. Technical report," 1999.

[13] A. Desolneux, L. Moisan and J. M. Morel, "Maximal Meaningful Events and Application to Image Analysis," *Annals of Statistics,* 2003, vol. 6, pp.1822-1828.

TABLE I. THE ITERATIVE DETECTION RESULTS

Block of blotch	Detection results				
	T_1=15	T_1=13	T_1=10	T_1=8	T_1=5
					
					
					
					
					
					

(a)

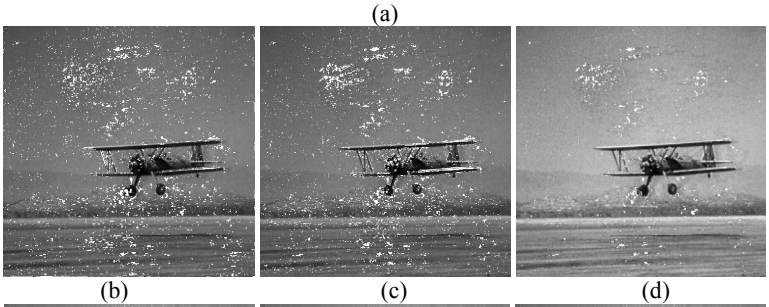

(b) (c) (d)

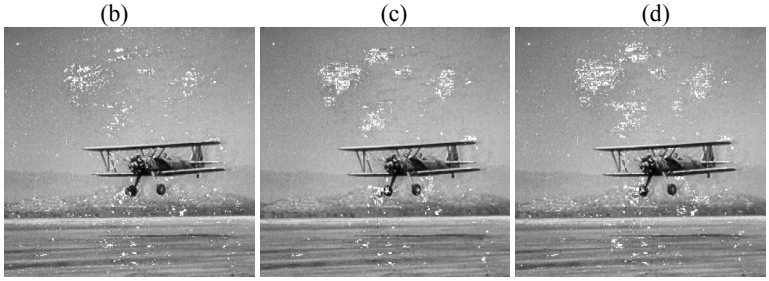

(e) (f) (g)

Fig. 7. The detection results of real degraded image sequence (a) the image sequence Bay with real degraded blotches (b) detection result of 2nd frame obtained by ROD with threshold 12 (c) detection result of 2nd frame obtained by SDIp with E_t 27 (d) detection result of 2nd frame obtained by S-ROD with threshold 15 (e) detection result of 2nd frame obtained by S-ROD with threshold 10 (f) detection result of 2nd frame obtained by our detector with threshold 15 (g) detection result of 2nd frame obtained by our detector with threshold 10

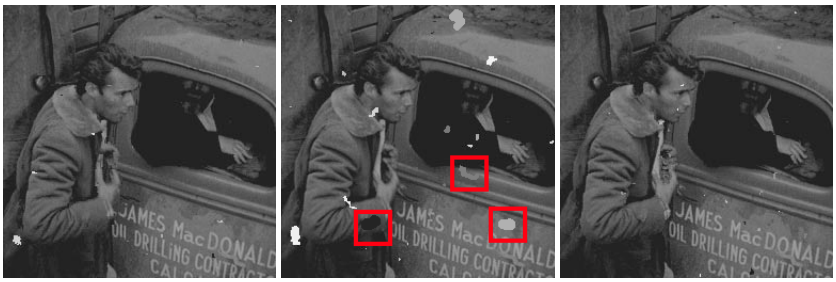

(a)

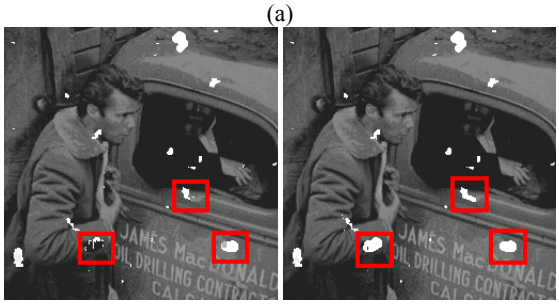

(b) (c)

Fig. 8. The detection results of random corrupted image sequence (a) the random corrupted image sequence Western (b) detection result of the 2nd frame obtained by S-ROD post detector with threshold 30 (c) detection result of the 2nd frame obtained by our detector with threshold 30

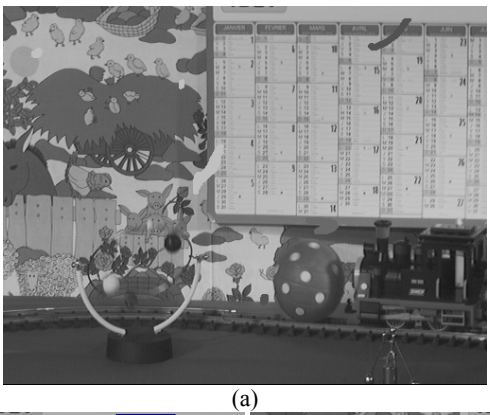

(a)

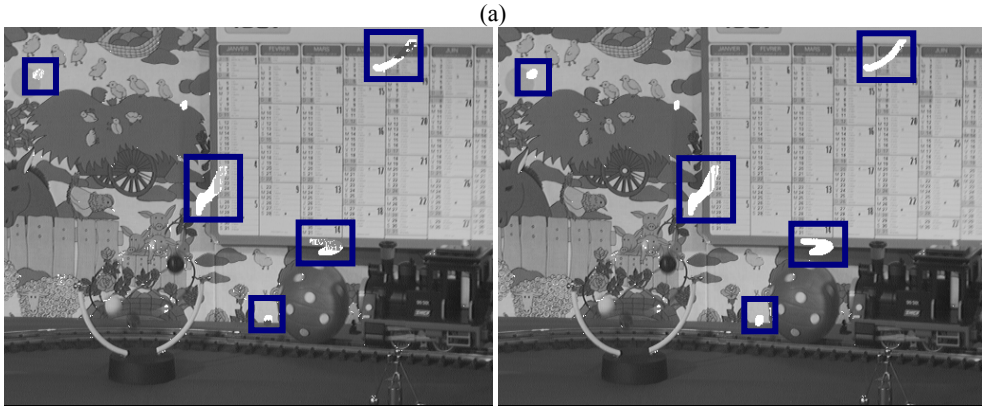

(b) (c)

Fig. 9. The detection results of artificial corrupted image sequence (a) the 2nd frame of Mobile and Calendar with artificial blotches (b) detection result obtained by S-ROD post detector with threshold 15 (c) detection result obtained by our detector with threshold 15

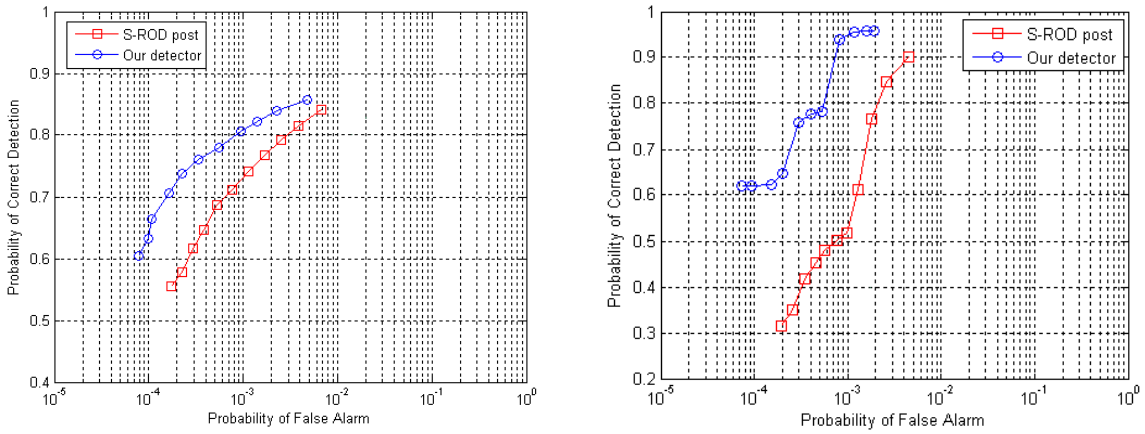

Fig. 10. ROC curves (a) performances of detectors applied to the Mobile and Calendar sequence with random corrupted blotches (b) performances of detectors applied to Fig. 9(a)